Size measurement method for Loblolly Pine grinds and influence on predictability of fluidization

Gbenga Olatunde[1], Oladiran Fasina[1], Sushil Adhikari[1], Timothy P. McDonald[1] and Steve R. Duke[2]

[1]*Department of Biosystems Engineering, Auburn University, Auburn, AL 36849 USA*
[2]*Department of Chemical Engineering, Auburn University, Auburn, AL 36849 USA*
Email: fasinoo@auburn.edu
http://dx.doi.org/10.7451/CBE.2016.58.4.1

Received: 2015 December 23, Accepted: 2016 March 9, Published: 2016 May 12.

Olatunde, G., O. Fasina, S. Adhikari, T.P. McDonald and S.R. Duke. 2016. **Size measurement method for Loblolly Pine grinds and influence on predictability of fluidization.** Canadian Biosystems Engineering/Le génie des biosystèmes au Canada **58**: 4.1-4.10. Biomass feedstocks are often fluidized in thermochemical conversion systems that are used to breakdown biomass into low molecular weight compounds. Fluidization equations such as Ergun equation are used to determine fluidization conditions by incorporating the values of the physical properties (e.g. diameter) of the material of interest in these equations. However, because biomass grinds have non-uniform and non-spherical particles, equivalent diameter values are dependent on the size measurement method. This study investigates how the equivalent diameters obtained from the size measurement methods affect the ability of five fluidization equations to predict the minimum fluidization velocities (U_{mf}) of fractions loblolly pine grinds. The behavior of loblolly pine wood grinds during fluidization was also assessed. Loblolly pine chips that were ground through 1/8" (3.18 mm) screen size were fractionated using six standard sieves that ranged between 0.15 mm and 1.7 mm. Particle density, bulk density, sphericities and equivalent diameters (based on minimum Feret, Martin, chord and surface-volume size measurement methods) for each fraction were measured. Size measurement method was found to significantly influence equivalent diameters of the grinds ($p < 0.05$). Highest value of equivalent diameter was obtained when minimum Feret diameter was measured. The U_{mf} of loblolly pine wood grinds (unfractionated samples) was found to be 0.25 ±0.04 m/s while the U_{mf} of fractionated samples increased with increase in particle size from 0.29 m/s to 0.81 m/s. The lowest mean relative deviation values of predicted U_{mf} from experimental U_{mf} was obtained when equivalent diameter from Martin diameter size measurement method was used in the fluidization equations.
Keywords: Particle size, measurement scheme, size distributions, biomass, fluidization, physical properties.

Les charges de biomasse sont fréquemment fluidisées dans des systèmes de conversion thermochimique qui sont utilisés pour réduire celles-ci en composés de petite masse moléculaire. Des équations de fluidisation, comme l'équation d'Ergun, sont employées pour déterminer les conditions de fluidisation en incorporant, dans ces équations, les valeurs des propriétés physiques (p. ex. diamètre) du matériau considéré. Cependant, parce que les moutures de la biomasse sont constituées de particules non uniformes et non sphériques, les valeurs de diamètre équivalent sont dépendantes de la méthode de mesure de taille. Ce projet étudie comment les diamètres équivalents obtenus par les méthodes de mesure de taille affectent la capacité de cinq équations de fluidisation à prédire les vélocités de fluidisation minimales (Umf) de moutures fractionnées de pin taeda. Le comportement des moutures de pin taeda a aussi été évalué pendant la fluidisation. Les copeaux de pin taeda ont été moulus à une taille de 1/8" (3,18 mm) et ils ont étaient fractionnés à l'aide de six tamis standards variant entre 0,15 mm et 1,7 mm. La masse volumique des particules, la masse volumique apparente, les sphéricités et les diamètres équivalents (basé sur les méthodes de mesure du minimum Feret, Martin, du diamètre tangentiel et de la taille surface-volume) pour chaque fraction ont été évalués. La méthode de mesure de taille s'est avérée avoir un effet significatif sur les diamètres équivalents des moutures ($p < 0,05$). La valeur de diamètre équivalent la plus élevée était obtenue lorsque le diamètre minimum Feret était mesuré. La Umf des moutures de pin taeda (échantillons non fractionnés) était de 0,25 ±0,04 m/s tandis que celles des échantillons fractionnés augmentaient de 0,29 m/s à 0,81 m/s avec la taille des particules. Les plus petites valeurs de déviation moyenne de Umf prédite des Umf expérimentales étaient obtenues lorsque le diamètre équivalent de la méthode de mesure de taille du diamètre Martin était utilisé dans les équations de fluidisation. **Mots clés:** taille de particule, système de mesure, distributions de taille, biomasse, fluidisation, propriétés physiques.

INTRODUCTION

Size reduction is an important preprocessing step in conversion of lignocellulosic biomass to fuels, products, and chemicals because the size of biomass feedstocks can be up to 100 fold of the particle size that can be efficiently and economically handled by biorefinery equipment. Size reduction however results in changes in the physical characteristics of biomass feedstock such as surface area, particle size and density (Mosier et al. 2005; Tumuluru et al. 2014). Biomass conversion efficiency, sizing of fluidized bed reactors, rate of heat and mass transfer, and estimation of particle residence time in thermo-chemical conversion processes are affected by these physical characteristics (Barakat et al. 2013; Schell and Hardwood 1994).

The particles that are produced during the size reduction of biomass feedstocks are non-uniform in size and non-spherical in shape. Fasina (2008) reported that the size range of peanut hulls ground through 3.18 mm screen was between 0.10 and 3.40 mm nominal sieve size. The size distribution was log normal with geometric mean diameter (d_{gw}) and geometric standard deviation (s_{gw}) of

0.65 and 0.75 mm respectively. Gil et al. (2013) used a hammer mill fitted with 2.0 mm screen size and obtained a d_{gw} and s_{gw} of 0.30 and 2.60 mm respectively for ground polar wood. Mani et al. (2004) reported that using hammer mill fitted with screen sizes that ranged between 0.8 and 3.2 mm, the particle density of wheat straw grinds varied between 1030 and 1340 kg/ m^3, barley straw grinds varied between 890 and 1250 kg/m^3, corn stover grinds varied between 1170 and 1340 kg/m^3, and switchgrass varied between 950 and 1170 kg/m^3. Adapa et al. (2009) measured the particle densities of ground wheat straw and ground canola straw to be between 1631 and 1539 kg/m^3, and 1504 and 1589 kg/m^3 respectively.

This non-uniformity in size, geometry, and density of biomass grinds impedes homogeneous mixing of bed during fluidization of these grinds. In addition, phenomena such as channeling, segregations, and plug flow have been attributed to the differences in the properties of the particles in the biomass grinds. For instance, Wang et al. (2015) fluidized seven fractions of sawdust and found that samples that passed through 0.25 mm screen, and those that were retained on 0.71 mm screen could not be properly fluidized because of channeling and slugging. Liu et al. (2008) observed that a mixture of glass ballotini (particle diameter of 0.57-0.24 mm and particle density of 2510-8750 kg/m^3) and coal (particle diameter of 2-40 mm and particle density of 1340 kg/m^3) segregate during fluidization because of substantial differences in the density and size of particles that constitute the bulk material. Also, Sharma et al. (2013) reported that channelization caused ineffective fluidization when gasifier residue (particle size of 0.080 mm), sand (particle size of 0.35 mm) and switchgrass grinds (particle size of 0.10 mm) were combined in a cold flow fluidization system (switchgrass was 5% of the feed on a mass basis).

Owing to the multi-sized nature of particles in biomass grinds, it is important to determine whether the fluidizing equations that have been used for other materials will be appropriate for biomass grinds fluidization. Five of these commonly used equations are listed below.

Ergun equation (Ergun 1952)

$$\frac{\Delta P}{L} = 150\frac{(1-\varepsilon)^2}{\varepsilon^3}\frac{\mu_g U_{mf}}{d_p^2} + 1.75\frac{(1-\varepsilon)}{\varepsilon^3}\frac{\rho_g U_{mf}^2}{d_p} \quad (1)$$

Modified Ergun equation (Ergun 1952)

$$\frac{\Delta P}{L} = 150\frac{(1-\varepsilon)^2}{\varepsilon^3}\frac{\mu_g U_{mf}}{(\phi_s d_p)^2} + 1.75\frac{(1-\varepsilon)}{\varepsilon^3}\frac{\rho_g U_{mf}^2}{(\phi_s d_p)} \quad (2)$$

Leva equation (Leva 1959)

$$U_{mf} = \frac{0.0093 d_p^{1.82}(\rho_p - \rho_g)^{0.94}}{\mu_g^{0.88}\rho_g^{0.06}} \quad (3)$$

Miller equation (Miller and Longwinuk 1951)

$$U_{mf} = 1.25\times10^{-3}\left(\frac{d_p^2(\rho_s - \rho_g)^{0.9}\rho_g^{1.1} g}{\mu_g}\right) \quad (4)$$

Geldart equation (Abrahamsen and Geldart 1980)

$$U_{mf} = 9\times10^{-4} d_p^{1.8}\left[(\rho_s - \rho_g)g\right]^{0.934}\rho_g^{-0.066}\mu_g^{-0.87} \quad (5)$$

where

U_{mf} = minimum fluidization velocity (m/s),
ρ_s = particle density (kg/m^3),
ρ_g = density of fluidizing gas (kg/m^3),
μ_g = dynamic viscosity of fluidizing gas (Pa s),
d_p = mean diameter of particle (m),
ε = void fraction of bed,
φ_s = sphericity of particle,
ΔP = pressure drop across bed (Pa),
L = height of bed (m),
g = acceleration due to gravity (m/s^2).

These fluidization equations require that the average diameter of the material to be fluidized be known. For spherical materials, a single diameter value is obtained by measuring the size, surface area, or volume of the particle. This is not the case for non-spherical particles such as biomass grinds. In particle technology, methods used to express the size of non-spherical particles include Martin, volume to surface area (i.e ratio of volume diameter to surface area diameter - also called Sauter mean), minimum Feret, and chord diameters (Rhodes 2008). Martin diameter is the length of chord through the centroid of the particle, which bisects area of the particle into two equal halves. The minimum Feret diameter is the smallest of the distance between pairs of parallel tangents touching opposite sides of the particle. Chord diameter is the distance between two points on the contour that is measured across the center of gravity of the projection area (Yang 2003). For the same non-spherical material, the magnitudes of the measured diameter from each of the diameter measurement method are different. The argument in literature has been that the choice of a diameter measurement method is influenced by the process/unit operation the material will be subjected to. For example, the surface-volume diameter is used in adsorption and reaction engineering because of the importance of exposed surface area to rate kinetics (Ortega-Rivas et al. 2006; Allen 1997). Expression of particle size in terms of Feret diameter, chord and Martin diameter has gained popularity in the past few years due to rapid and non-destructive nature of imaging (optical and microscopy) techniques when used to obtain size distribution of materials. One advantage of these three diameter expressions is that they are statistical in nature because each of the particles in a sample will take a random orientation during size measurement (Iinoya et al. 1988; Ortega-Rivas et al. 2006). However, there is no evidence in scientific literature regarding the use of Feret, Martin, or chord diameter in fluidizing equations especially because thee equivalent diameters are statistical representative of the size of the particles in a ground sample.

Table 1. Effect of size measurement method on the d_{50} - equivalent diameter (mm) of unfractionated (sample A) and fractionated (sample B series) loblolly pine grinds.

Sample	Sieve range*	Sieve opening (mm)	Chord	Min. Feret	Martin	Surf-volume
A	-	-	1.00[b]	1.07[a]	0.83[c]	0.79[c]
B1	>12	> 1.7	2.11[b]	2.24[a]	1.83[c]	1.83[c]
B2	12-14*	1.7 – 1.4	1.68[b]	1.80[a]	1.42[b]	1.47[b]
B3	14-18	1.4 – 1.0	1.39[b]	1.49[a]	1.10[d]	1.19[c]
B4	18-30	1.0 – 0.6	1.04[b]	1.13[a]	0.80[d]	0.84[c]
B5	30-50	0.6 – 0.3	0.63[b]	0.69[a]	0.52[c]	0.45[d]
B6	50-100	0.3 – 0.15	0.55[a,b]	0.59[a]	0.45[c]	0.24[d]

*for example, 12-14 implies sample B2 passed through sieve #12 and was retained on sieve #14.

Values are d_{50} from the particle size distribution data and are mean of three replicates.

Means with different letters in a row are significantly different ($p<0.05$)

Furthermore, the equations used for predicting fluidization velocity were based on average values of material properties such as density, sphericity and particle diameter. These equations were developed with the underlying principle that mono-component bed having a uniformly sized particle is being fluidized. Several studies in the literature have documented that this assumption is responsible for the significant deviation of experimentally determined fluidization velocities for biological materials from predicted values (Rao et al. 2001; Aznar et al. 1992). Therefore, the ability of commonly used equations to predict the minimum fluidization velocities of non-uniformly sized and non-spherical materials must be examined.

In this study, particle properties (particle & bulk density, porosity, shape, and size distribution) of loblolly pine wood grinds were quantified with the particle size being determined based on chord, Feret, and Martin size measurement method for fractionated and unfractionated loblolly pine grind. The measured properties were incorporated into five fluidization equations (Eqns 1 to 5) with the goal of predicting the U_{mf} of loblolly pine wood grinds and comparing the predicted to the experimentally determined U_{mf}. Fractionated samples were used to study the influence of particle size distribution and the suitability of each size measurement method to predict minimum fluidization velocity of loblolly pine grinds. The occurrence of channel, plug flow and de-fluidization during fluidization of the various samples of loblolly pine grinds was also assessed.

MATERIALS AND METHODS

Sample preparation

Loblolly pine wood chips were obtained from trees harvested in a forest plantation in Alabama, U.S. The chips were air-dried for about 2 weeks followed by grinding with a hammer mill (model 10 HBLPK, Sheldon Manufacturing, Tiffin, OH) fitted with 3.18 mm diameter round holes screen. After grinding, the moisture content of the sample was determined to be 8.4% (wet basis) by using ASTM standard E871-82 procedure (ASTM 2013) that involves placing about 10 g sample in a convective oven at 105±2°C for 24 hrs.

The ground samples were divided into two groups: unfractionated (sample A) and fractionated (sample B series). To prepare the sample B series, about 100 g of loblolly pine grinds was fractionated into six fractions using combination of six sieves (Table 1) that were placed on a sieve shaker (model Rx 29, Tyler, Inc., Mentor, OH). The shaker was operated for 15 minutes. The fractionation process was repeated until an average mass of 1.5 kg was obtained for each fraction. These fractionated samples (i.e. sample B series) and sample A were fluidized after the determination of their physical characteristics.

Particle size analysis

Particle size analysis was carried out on 100 g of samples A and B with a volume based image analysis system (Camsizer®, Retsch Technology, Haan, Germany). The software provided by the equipment manufacturer was used to measure the Martin, chord and minimum Feret diameters (i.e. d_{50} – the 50% probability diameter which is the diameter at which 50% of the particles in a sample is comprised of smaller particles). The software was also used to obtain the average specific surface area (S_{ssa}) and mean sphericity (φ) values of these samples using the chord diameter measurement method since the chord diameter is the default method that Camsizer uses to measure sample diameter. S_{ssa} was then used to calculate the surface to volume equivalent sphere diameter d_{sv} (Eqn. 1) (Rhodes 2008).

$$d_{sv} = \frac{6}{S_{ssa}} \tag{6}$$

Particle density, bulk density and porosity

A gas pycnometer (Accupyc 1330, Micromeritics Instrument Corp., Norcross, GA) was used to measure the particle densities of the samples. The gas pycnometer, uses helium to estimate the pressure difference between a reference cell and a cell containing the sample. The pressure difference was used by the pycnometer to estimate the volume of a known mass of sample. The particle density was computed using Eqn. 7.

$$\rho_p = \frac{m_p}{v_p} \tag{7}$$

where, ρ_p is particle density (kg/m^3), m_p is sample mass (kg) of particle, and v_p is sample volume (m^3) of particle.

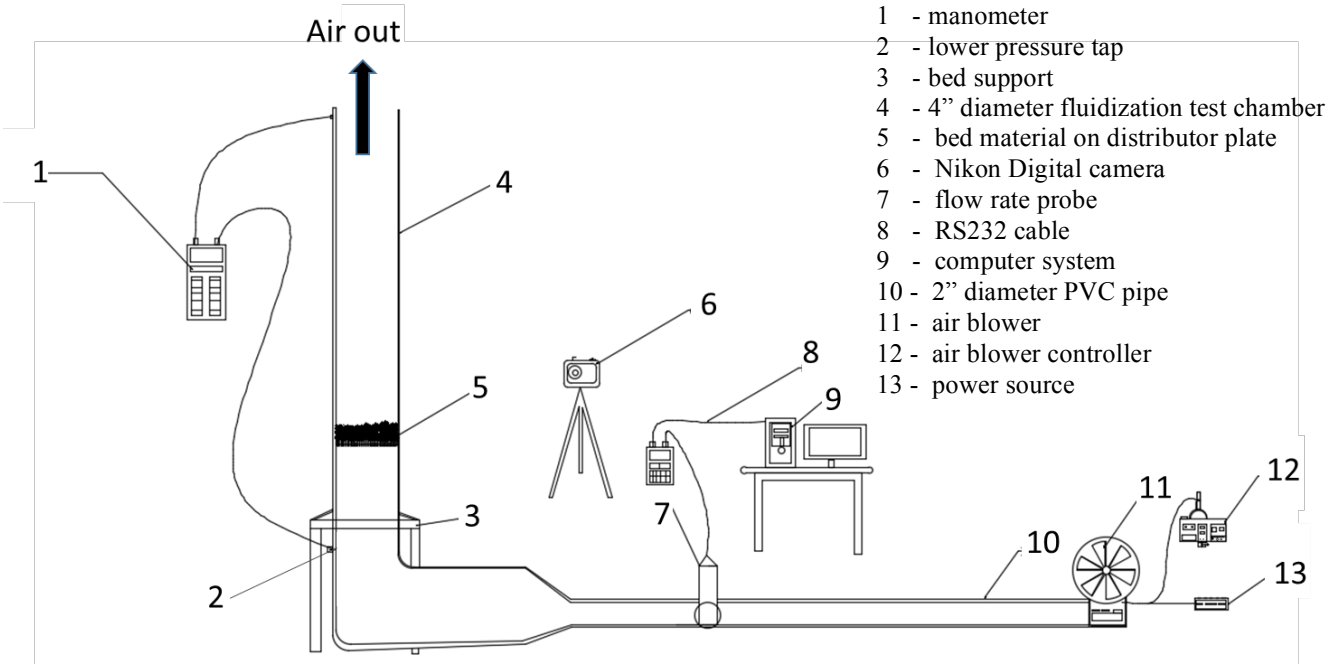

Fig. 1. Schematic diagram of the system used for fluidization.

Bulk densities of all the samples were determined using an apparatus that consists of a funnel through which the sample freely falls onto 1137 mm^3 cup. Bulk density was estimated as the ratio of the mass of the sample in the container to the volume of the container. The inter-granular porosity (ε) of each sample was calculated from the measured values of bulk density and particle density as follows;

$$\varepsilon = 1 - \frac{\rho_b}{\rho_p} \quad (8)$$

where, ρ_b is bulk density (kg/m^3).

Fluidized bed and fluidization test

Figure 1 shows a schematic diagram of the fluidized bed system that was used to measure the minimum fluidization velocity of the samples. The bed is composed of an acrylic cylindrical pipe with internal diameter of 101.6 mm and a height of 1000 mm. The system was also fitted with a distributor that has 100 µm uniformly distributed perforations (Purolator, Model UNS 530403, Sacramento, CA). The distributor supported the samples to be fluidized. Fluidized gas (air) was supplied by a blower (Black and Decker, Model LH5000, Antioch, CA). Air speed was regulated by a fan speed controller (Lutron electronic, MFG part S2-LFSQH-WH Monroe, NJ) and measured by a vane anemometer (FM Metal Vane anemometer, model 407113, Nashua, NH) located at 0.7 m from the blower. The anemometer readings were transmitted to and recorded by a personal computer via a RS-232 interface. The software (Vane anemometer data logger, model 47001, version 4.0) provided by the manufacturer was used to display the airflow rate on the computer monitor.

Pressure drop across the bed was measured by connecting a U-tube manometer into the upper (800 mm above the distributor) and lower (200 mm below the distributor) pressure taps. In order to quantify the pressure drop across the distributor at no load conditions, the pressure drop (ΔP_{empty}) across the bed and the corresponding air velocity were respectively measured and

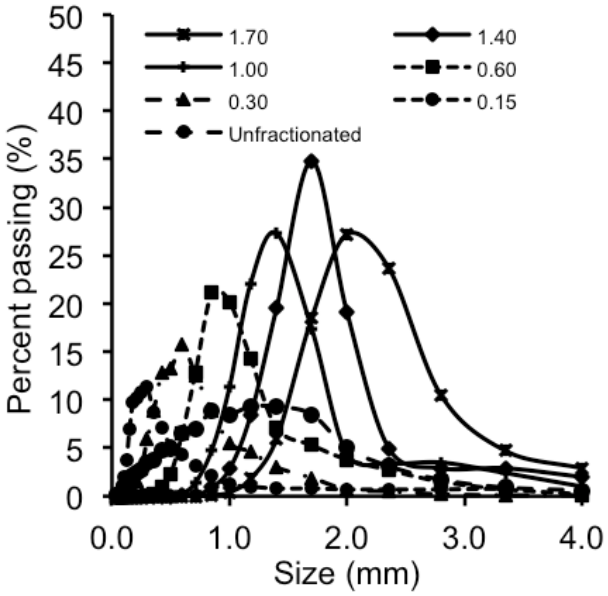

Fig. 2. Particle size distribution of fractionated and unfractionated ground loblolly pine wood. *Numbers in the legend are the nominal diameters (mm) of the screen used for fractionation.

Table 2. Physical characteristics and experimentally determined minimum fluidization velocity (U_{mf}) of unfractionated (sample A) and fractionated (sample B series) loblolly pine grinds.

Sample	Sieve range	Bulk density (kg/m^3)	Particle density (kg/m^3)	Porosity	Sphericity	U_{mf} (m/s))
A	-	311.1^{a}	1469.0^{c}	0.79^{e}	0.52^{d}	0.250±0.04
B1	>12	278.0^{c}	1471.6^{b}	0.92^{c}	0.60^{a}	0.805±0.007
B2	12-14	277.7^{c}	14661^{c,b}	0.81^{c}	0.57^{b,a}	0.625±0.035
B3	14-18	320.7^{a}	1470.7^{b}	0.78^{e}	0.55^{b,c}	0.525±0.11
B4	18-30	290.3^{b}	1468.2^{c,b}	0.79^{d}	0.51^{c,d}	0.400±0.07
B5	30-50	234.3^{d}	1486.9^{a}	0.84^{b}	0.41^{e}	0.265±0.02
B6	50-100	169.3^{e}	1512.7^{a}	0.89^{a}	0.23^{e}	0.290±0.01

Means with different letters in a column are significantly different ($p<0.05$)

recorded with the manometer and vane anemometer. The flow patterns and bed mixing behavior at different operating conditions were studied from recordings made with a digital camera (Nikon, Model S3100 Melville, NY) that was installed in front of the fluidized bed.

To obtain the fluidization data for a sample, a weighed sample (120 g) was poured on the distributor of the fluidization system. The blower was turned on and the fan speed controller was used to increase the velocity of air flowing into the bed until a desired air velocity was attained. After 60 s (for stabilization of flow), pressure drop (ΔP_{Total}) across the sample bed, and the airflow rate were recorded. Minimum fluidization velocity was estimated from the pressure drop versus air velocity rate plot according to the procedure outlined by Kunii and Levenspiel (1991) and Gupta and Sathiyamoorthy (1998). To verify accuracy of the readings (pressure and airflow rate) obtained from this study, the fluidization system was used to measure the minimum fluidization velocity of sand.

Data analysis

All experiments were conducted in triplicates. The results were presented in relevant section as mean values and standard deviation. The effect of sample size obtained from the different size measurement scheme on particle size diameter, bulk density, particle density, porosity and sphericity factor were analyzed using the generalized linear model in SAS statistical software (SAS, 2014). In addition, the Tukey test was used to compare means at $p \leq 0.05$. The closeness of the predicted (minimum fluidization velocity based on equations and diameter types) and observed (minimum fluidization velocity obtained from laboratory experiment) was assessed using mean relative deviation (MRD) (Nemec and Levec 2005).

$$MRD(\%) = \frac{1}{N} 100 \sum_{i=1}^{N} \frac{\left| \lambda_{1.calc} - \lambda_{i.\exp} \right|}{\lambda_{i.\exp}} \quad (9)$$

where

$\lambda_{1.calc}$ = calculated U_{mf} from fluidization equation (m/s),

$\lambda_{i.\exp}$ = experimentally determined U_{mf} (m/s),

N = numbers of data points.

RESULTS AND DISCUSSION

Particle size

Particle size distributions (based on chord diameter) for the unfractionated (sample A) and the six fractionated loblolly pine grinds (sample B series) are shown in Fig 2. There was skewness in the distributions of all the samples, which is typical of ground biological materials (Fasina 2006). Figure 2 also shows that there are substantial portion of the particles in loblolly pine grinds (sample A) are in dust form (i.e. particle size less than 0.5 mm – NFPA 2007). Dust that is generated during the preprocessing of biomass is responsible for clogging of filters, and for fire and explosion hazards in biomass processing plants (Kenney et al. 2013; Hehar et al. 2014). In addition, the reduction in flowability of biomass grinds with decrease in particle size further supports the influence of the finer fractions of biomass grinds on fluidization behavior (Littlefield et al. 2011; Gil et al. 2013).

Table 1 shows that irrespective of the size measurement method, the d_{50} diameter of sample B series are larger than the size of the screen used to fractionate the sample thus confirming the visual observation of the elongated nature of loblolly pine grinds. Limited analysis on the size data obtained from the image analysis system show that the aspect ratio values for the grinds were about 2.5. Table 1 also shows that the values of the diameters were significantly ($P<0.05$) affected by the method using to measure particle diameter. This affirms the non-spherical nature of loblolly pine grind particles. For all samples, the highest diameter values were obtained from the minimum Feret diameter measurement method. Lowest diameter values were obtained from Martin diameter method for samples that were retained on screens with apertures larger than 0.3 mm, and from surface volume diameter method for samples retained on screens smaller than 0.3 mm. Further analysis (Table 2) shows that the sphericity of the particles reduces with reduction in particle size. The measured Martin diameter (which is length of chord that bisects a particle into two equal halves) is therefore reflecting the lower sphericity of the smaller particles.

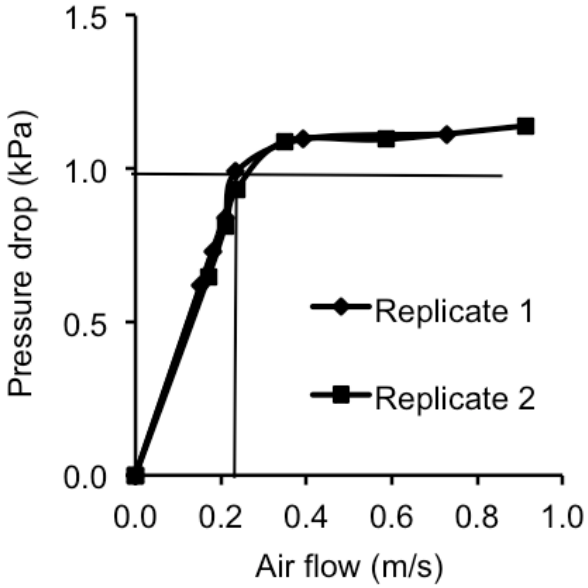

Fig. 3. Plot of pressure drop versus air velocity for sand particles.

Particle density, bulk density and porosity

There were no trends between particle densities and particle size of fractionated samples (Table 2). This suggests that voids within individual particle were not affected by the grinding (through 3.12 mm screen size) process and by particle size. The particle density of the unfractionated sample was 1469.5 kg/m^3 which is similar to the value of 1440.0 kg/m^3 reported by Hehar et al. (2014) for loblolly pine wood grinds. The bulk density of unfractionated sample was found to be 311 kg/m^3 while those of the fractionated samples significantly increase from 166 kg/m^3 to 278 kg/m^3 as particle size increased. Fig. 2 shows that the spread of the size distribution increased with increase in screen size. Since particle shape and orientation of particles affect inter-granular spaces, when particles of wide distribution are poured into a container, smaller particles occupy spaces between bigger particles. This we believe is responsible for the increase in bulk density as screen size increased.

Table 2 also shows that the porosity of the grinds varied between 0.78 and 0.91, and that porosity initially decreased with increase in particle size up and then increased with further increase in particle size. The minimum pore space was obtained from samples that were retained on 1.0 mm screen. Similar high values of pore space were reported by Lam et al. (2008) who found that the porosity of switchgrass increased from 0.82 to 0.87 as particle size decreased from 2.00 mm to 0.10 mm. Unfortunately, these high void fractions may contribute to channeling formation during fluidization.

Validation of fluidization setup

Based on the plot of pressure drop across against the air velocity when the fluidization bed contains sand (Fig. 3), the minimum fluidization velocity (U_{mf}) of sand was measured to be 0.28 ± 0.002 (m/s). The minimum fluidization velocity was identified as the intersection between the rising and constant bed pressure drop (Gupta and Sathiyamoorthy 1998). It can be seen from Fig. 3 that duplicate runs for the sample are essentially the same. Patil et al. (2005) measured the U_{mf} of sand to be 0.34 m/s. This validates the pressure drop – velocity data obtained from the fluidization setup of Fig. 1.

Fig. 4. Picture shows example of channeling during fluidization of loblolly pine grinds.

Fluidization behavior of Loblolly Pine grinds

Fig. 4 shows that channeling occurred during fluidization of the samples most likely because of the high pore space in loblolly pine grinds. Smaller particles were entrained in the air stream when airflow through the bed reached a velocity (around 0.16 to 0.30 m/s) at which the updraft created from the airflow was sufficient to lift the bed entirely. The entrained particles were either deposited in another location in the bed or carried out of the bed. This rearrangement caused the airflow to concentrate in a particular region (region that offered least resistance to airflow) thus causing channels of various sizes, which can vary from multiple small channels (less than 0.01m diameter) to a channel with diameter that is almost 50% of the diameter of the bed. This process of reoccurrence of channel formation was more frequent in the larger sized fractions (unfractionated sample and fractions that were retained on screens with apertures equal or greater than 1.0 mm). Channel formation in larger particles could be attributed to the relative ease in which the air passes through the interconnected void within the large particles.

Table 3. Mean relative deviation (%) between experimentally determined U_{mf} and calculated U_{mf} from five fluidization equations (Eqns. 1 to 5).

Sample	Size method	d_{50} (mm)	Ergun	Mod-Ergun	Leva	Miller	Geldart
A	Chord	1.01	168.2	252.8	38.9	72.3	21.8
	Min. Feret	1.07	174.6	261.7	48.8	87.2	29.6
	Martin	0.83	147.7	224.5	12.2	32.6	0.4
	Surf. vol	0.79	142.9	217.8	6.9	24.8	-3.8
B1	Chord	2.11	-85.3	-121.9	-66.2	-126.4	-44.4
	Min. Feret	2.24	-89.2	-126.8	-78.4	-147.6	-54.0
	Martin	1.83	-76.7	-110.7	-41.9	-85.2	-25.3
	Surf. Vol	1.83	-76.7	-110.7	-41.9	-85.2	-25.3
B2	Chord	1.68	-72.9	-108.0	-34.6	-69.7	-20.6
	Min. Feret	1.80	-76.7	-113.0	-43.9	-85.2	-27.9
	Martin	1.42	-64.2	-96.5	-16.2	-39.8	-6.1
	Surf. vol	1.47	-66.1	-98.8	-19.0	-45.2	-8.7
B3	Chord	1.39	-58.3	-89.1	-18.5	-40.6	-8.9
	Min. Feret	1.49	-61.4	-93.3	-25.0	-51.1	-14.1
	Martin	1.10	-48.5	-75.9	-1.6	-14.2	4.4
	Surf. Vol	1.19	-51.7	-80.2	-6.5	-21.7	0.6
B4	Chord	1.04	-47.3	-74.3	-8.2	-19.1	-2.8
	Min. Feret	1.13	-50.2	-78.3	-12.9	-26.1	-6.5
	Martin	0.80	-39.0	-62.7	2.4	-3.1	5.7
	Surf. vol	0.84	-40.4	-64.7	0.8	-5.5	4.4
B5	Chord	0.63	-30.4	-56.1	3.6	0.6	5.7
	Min. Feret	0.69	-32.5	-59.4	1.5	-2.2	4.0
	Martin	0.45	-23.3	-45.0	8.8	7.6	8.4
	Surf. Vol	0.45	-23.3	-45.0	8.8	7.6	9.9
B6	Chord	0.55	-18.4	-55.2	6.1	4.0	7.7
	Min. Feret	0.59	-19.6	-57.7	4.9	2.4	6.7
	Martin	0.52	-17.5	-53.3	7.0	5.2	6.6
	Surf. vol	0.24	-6.6	-31.3	13.0	12.9	13.3

Kunii and Levenspiel (1991) suggested that the presence of fine particles in a sample can be used to increase airflow resistance and reduce the easy formation of channels during fluidization because of the redirection of airflow by the fine particles.

Further increase in air velocity resulted in bigger particles settling at the base in an interlock position. In between the interlocked particles (mostly bigger particles) are trapped smaller particles that made air penetration through the bed difficult. All of these rearrangements of particle resulted in the bed rising in a plug. Increasing the airflow rate disentangled the plugs. Defluidization was another phenomenon that was observed after complete fluidization velocity of bed was achieved. Defluidization occurs after significant entrainment of smaller particles from the bed. Therefore, the remaining large particles require higher flow rate to fluidize. At this particular condition, a multi-component bed was turned into a mono-component bed.

Experimental determination of minimum fluidization velocity (U_{mf})

The plot of pressure drop against air velocity for sample A (unfractionated) and samples from group B fractionated (sample B) is shown in Fig. 5. In an ideal situation, the pressure drop should not increase after the onset of fluidization i.e. minimum fluidization velocity is obtained at the intersection of the increasing pressure drop line (representing fixed bed) and the constant pressure drop line (representing fixed bed). However, due to forces such as particle-to-particle cohesive force, particle-wall interactions, non-uniformity in sizes of particles (Srivastava and Sundaresan 2002) and the rearrangement of bed as described in the last section, increase in pressure drop occurs after the onset of fluidization was visually observed. We therefore used the weight (based on mass of sample) per unit area (i.e. cross-sectional area of fluidization bed) approach to determine the minimum fluidization velocity. This approach has also been used by

other researchers in situations where the minimum fluidization velocities are difficult to estimate from the pressure drop versus air velocity curves (Kunii and Levenspiel 1991; Srivastava and Sundaresan 2002). The minimum fluidization velocity was obtained by computing the weight per unit area (W/A) for each sample and finding the air velocity that correspond to the calculated W/A (i.e. pressure drop) on the pressure drop – air velocity curve for that sample. It should be mentioned that the extent of the wobbling of the pressure drop-air velocity plot decreased with narrower size distribution thus confirming that non-uniformity in particle size may be contributing to the wobbling nature of the curves.

The minimum fluidization velocity of sample 'A' (unfractionated sample) was measured to be 0.25±0.04 m/s. All of the 'B' samples have U_{mf} greater than 0.25 m/s (the minimum fluidization velocity of unfractionated sample) with the minimum fluidization of larger particles being about 3 times that of the smaller particles (Table 2). This explains the reason why large particles in ground samples remain un-fluidized whereas smaller particles are fluidized and often ejected out of fluidization chamber. Similar observation was made by Liu eta al. (2008) when coal samples (size between 0 mm and 40 mm) were mixed and fluidized at a superficial gas velocity of 3.0 m/s for 10 min. They found that the coal samples behave as a pseudo binary mixture of particles in the 0-10 mm range and 10-40 mm range. In addition, 45% of the sample remained at the bottom fluidization reactor (i.e. large particles that did not fluidize). A significant amount (28%) of the initial sample elutriate out of the fluidization chamber.

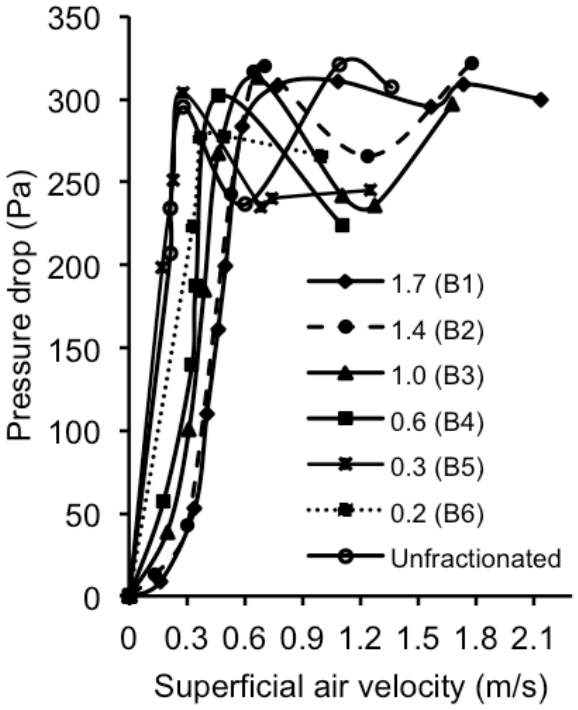

Fig. 5. Pressure drop versus superficial air velocity for unfractionated (sample A) and fractionated (sample B series) loblolly pine grinds. (*Numbers in the legend are the nominal diameters (mm) of the screen used for fractionation.)

Prediction of minimum fluidization velocity

The predicted minimum fluidization (U_{mf}) velocity for each sample was obtained by inserting the appropriate values of the properties of the samples in the five fluidization equations presented earlier (Eqns. 1 to 5). In addition, Umf was estimated based on equivalent diameters obtained from each diameter measurement method - Martin, chord, geometric mean, minimum Feret, and surface-volume diameter. The predicted minimum fluidization velocities obtained from these equations were then compared to the experimentally determined velocities for each sample (Tables 1 and 3). Mean relative deviations (MRD) of Eqn. 9 was used as a measure of the closeness of the predicted to the experimental U_{mf} values.

For unfractionated sample (sample A), Miller had the least deviation irrespective of the measurement scheme but predictions obtained from Ergun equations (Ergun and Mod-Ergun) were significantly different from other equations. For instance, using surface to volume diameter, the MRD obtained from Ergun and Mod-Ergun was 142.9 and 217.8 % respectively while Leva, Miller, and Geldart equation was 6.9, 24.8 and -3.85 % respectively. Geldart, Leva, and Miller equation were developed through experimental correlations and have similar structure as depicted in Eqn. 10 while Ergun equations were developed based on frictional force (due to viscous and kinetic energy) in a packed bed that is composed of uniformly sized particles. In addition, Ergun equation requires that more of the properties (e.g. porosity and sphericity) of the material being fluidized be known. This probably increased the error obtained. For instance, a constant porosity value was assumed in estimating U_{mf} even though several authors and observation from this study show that bed porosity changes with velocity (Vejahati et al. 2009).

$$U_{mf} = \frac{K d_m^l \left(\rho_p - \rho_g\right)^x}{\mu_g^n \rho g^y} \quad (10)$$

where, k, l, x, n and, y represent different coefficient obtained from the fitting process.

For fractionated samples (sample B series), the deviation between predicted from each equation and experimental data reduced with reduction in particle size. As mentioned before, the smaller the particle size, the narrower the size distribution (Fig. 2). Therefore the diameter used in the equations is more representative of the total particles in a sample as the average diameter of the sample reduces. When the sample size was larger than 1.00 mm, Geldart equation produced the least MRD values irrespective of the method used to measure particle size. The least MRD was obtained from Leva equation for the remaining fractions (i.e. with particles less than 1.00 mm). It should be mentioned that the MRD values obtained from

Leva, Geldart and Miller equations, were less than 15% when the samples were less than 1.00 mm. This again indicates that size distribution plays a prominent role in the ability of fluidization equation to predict U_{mf}.

Surprisingly, the Ergun equation predicted better than the modified Ergun equation despite the incorporation of sphericity (or shape factor) in the modified Ergun equation. Therefore, it can be deducted from this study that adjusting Ergun equation with a shape factor is not as important as using the equation that captures the behavior of non-uniformly sized particles during fluidization. This may require that the Ergun equation be refitted with fluidization data for non-uniformly size particles. Also, the MRD values obtained from the fit of the Ergun equations were not a strong function of the method used to measure particle size when compared to the MRD values obtained Miller, Leva and Geldart equations. This implies that if Ergun can be refitted, it would be a better equation to predict U_{mf} of multicomponent particles.

The predicted U_{mf} values using the Martin method of measuring diameter were generally the closest to the experimental U_{mf} values. We believe that this is because of the interrelationship between buoyancy force (one of the forces acting on a particle suspended in a fluid system), the centroid of the particle and fluidization. The centroid a particle is used in estimating the Martin diameter and the line of action of buoyancy force acting on a particle is also through the centroid of the particle. Fluidization occurs when the sum of the buoyancy force and drag force acting on a particle is greater than the weight of the particle (McCabe et al. 2005.). Predictions from use of surface-volume diameter in the equations were however not significantly different from the Martin method. Since biomass grinds are not typically fractionated, Martin diameter can be used to predict Umf when imaging technique is available to measure particle size. In situations where sieve analysis method is the only method available to measure particle size, a reliable prediction of Umf can be obtained by computing and using the surface-volume diameter estimated from the sieve analysis method.

CONCLUSIONS

It can be concluded from this study that:

1. The choice of size measurement method has significant impact on the equivalent diameter of samples that have non-uniform size and that are non-spherical in shape. Specifically, for loblolly pine grinds, the minimum Feret diameter was higher than surface-volume, Martin and chord diameters by 18.3, 23.6, and 7.03% respectively.
2. The minimum fluidization velocity (U_{mf}) of unfractionated loblolly pine wood grinds was measured to be 0.25 ±0.04 m/s) while U_{mf} of fractionated sample increased with increase in particle size from 0.29 m/s to 0.81 m/s.
3. Values of diameters obtained from the different size measurement method significant impact the ability of fluidization equations to predict minimum fluidization of loblolly pine grinds. Martin diameter generally exhibited the least MRD values. It is therefore recommended for use in equations for predicting minimum fluidization velocity.

ACKNOWLEDGEMENT

We gratefully acknowledge funding support from USDA-NIFA project through the Southeast Partnership for Integrated Biomass Supply Systems (IBSS).

REFERENCES

Abrahamsen, A. and D. Geldart. 1980. Behaviour of gas-fluidized beds of fine powders part I. homogeneous expansion. Powder technology 26: 35-46. http://dx.doi.org/10.1016/0032-5910(80)85005-4

Adapa, P., L. Tabil and G. Schoenau. 2009. Compaction characteristics of barley, canola, oat and wheat straw. Biosystems Engineering 104: 335-344. http://dx.doi.org/10.1016/j.biosystemseng.2009.06.022

Allen, T. 1997. Particle Size Measurement Volume 2: Surface Area and Pore Size Determination. London, UK: Chapman and Hall.

ASTM 2013. ASTM E871-72: Standard test methods for moisture analysis of particulate wood fuels. American Society for Testing Materials. West Conshohocken, PA: ASTM International.

Aznar, M.P., F.A. Gracia-Gorria and J. Corella. 1992. Minimum and maximum velocities for fluidization for mixtures of agricultural and forest residues with a second fluidized solid. II. Experimental results for different mixtures. International Chemical Engineering 32: 103-113.

Barakat, A., H. de Vries and X. Rouau. 2013. Dry fractionation process as an important step in current and future lignocellulose biorefineries: A review. Bioresource Technology 134: 362-273. http://dx.doi.org/10.1016/j.biortech.2013.01.169

Ergun, S. 1952. Fluid flow through packed columns. Chemical Engineering Progres 48: 89-94.

Fasina, O. 2006. Flow and physical properties of switchgrass, peanut hull, and poultry litter. Transaction of ASABE 49: 721-728. http://dx.doi.org/10.13031/2013.20470

Fasina, O.O. 2008. Physical properties of peanut hull pellets. Bioresource Technology 99: 1259-1266. http://dx.doi.org/10.1016/j.biortech.2007.02.041

Gil, M., D. Schott, I. Arauzo and E. Teruel. 2013. Handling behavior of two milled biomass: SRF poplar and corn stover. Fuel Processing Technology 112: 76-85. http://dx.doi.org/10.1016/j.fuproc.2013.02.024

Gupta, C.K. and D. Sathiyamoorthy. 1998. Fluid Bed Technology in Materials Processing. New York, NY: CRC Press. http://dx.doi.org/10.1201/9781420049862

Hehar, G., O. Fasina, S. Adhikari and J. Fulton. 2014. Ignition and volatilization behavior of dust from loblolly pine wood, Fuel Processing Technology 127: 117-123. http://dx.doi.org/10.1016/j.fuproc.2014.04.036

Iinoya, K., H. Masuda and K. Watanabe, 1988. Powder and Bulk Solids Handling Processes: Instrumentation and Control. Boca Raton, FL: CRC Press.

Kenney, K.L., W.A. Smith, G.L. Gresham and T.L. Westover. 2013. Understanding biomass feedstock variability. Biofuels 4: 111-127. http://dx.doi.org/10.4155/bfs.12.83

Kunii, D. and O. Levenspiel. 1991. Fluidization Engineering. Boston, MA: Butterwrth-Heinemann Publishing Company.

Lam, P., S. Sokhansanj, X. Bi, C. Lim, T. JayaShankar, G. Rezaie and L. Naimi. 2008. The effect of particle size and shape on physical properties of biomass grinds. ASABE Meeting Presentation Paper 080014.

Leva, M. 1959. Fluidization. London: McGraw-Hill Book Company.

Littlefield, B., O. Fasina, J. Shaw, S. Adhikari and Via, B. 2011. Physical and flow properties of peacn shells – particle size and moisture effects. Powder Technology 212: 173.180. http://dx.doi.org/10.1016/j.powtec.2011.05.011

Liu, X., G. Xu and S. Gao. 2008. Fluidization of extremely large and widely sized coal particles as well as its application in an advanced chain grate boiler. Powder Technology 188: 23-29. http://dx.doi.org/10.1016/j.powtec.2008.03.008

Mani, S., L.G. Tabil, and S. Sokhansanj. 2004. Grinding performance and physical properties of wheat and barley straws, corn stover and switchgrass. Biomass and Bioenergy 27: 339-352. http://dx.doi.org/10.1016/j.biombioe.2004.03.007

McCabe, W.L., J.C. Smith and P. Harriott. 2005. Unit Operations of Chemical Engineering. New York: McGraw-Hill Book Company.

Miller, C.O. and A. Logwinuk. 1951. Fluidization studies of solid particles. Industrial and Engineering Chemistry 43: 1220-1226. http://dx.doi.org/10.1021/ie50497a059

Mosier, N., C. Wyman, B. Dale, R. Elander, Y.Y. Lee, M. Holtzapple and M. Ladisch. 2005. Features of promising technologies for pretreatment of lignocellulosic biomass. Bioresource Technology 96: 673-686. http://dx.doi.org/10.1016/j.biortech.2004.06.025

Nemec, D. and J. Levec. 2005. Flow through packed bed reactors: 1. Single-phase flow, Chemical Engineering Science. 60: 6947-6957. http://dx.doi.org/10.1016/j.ces.2005.05.068

NFPA. 2007. Guide for venting of deflagrations. NFPA 68. Qunicy, MA: National Fire Protection Association.

Ortega-Rivas, E., P. Juliano and H. Yan. 2006. Food Powders: Physical Properties, Processing, and Functionality. New York, NY: Springer.

Patil, K., T. Bowser, D. Bellmer and R. Huhnke. 2005. Fluidization characteristics of sand and chopped switchgrass-sand mixtures. International Commission of Agricultural Engineering (CIGR) e-Journal, 7.

Rao, R.,T. Ram and J.V. Bheemarasetti. 2001. Minimum fluidization velocities of mixtures of biomass and sands. Energy 26: 633-644. http://dx.doi.org/10.1016/S0360-5442(01)00014-7

Rhodes, M. 2008. Introduction to Particle Technology, 2nd edition. West Sussex, England: John Wiley and Sons. http://dx.doi.org/10.1002/9780470727102

SAS. 2014. The SAS system for Windows, SAS Institute, Cary, NC.

Schell, D. and C. Harwood. 1994. Milling of lignocellulosic biomass. Applied Biochemistry and Biotechnology 45-46: 159-168. http://dx.doi.org/10.1007/BF02941795

Sharma, A.M., A. Kumar, K.N. Patil and R.L. Huhnke. 2013. Fluidization characteristics of a mixture of gasifier solid residues, switchgrass and inert material. Powder Technology 235: 661-668. http://dx.doi.org/10.1016/j.powtec.2012.11.025

Srivastava, A. and Sundaresan, S. 2002. Role of wall frcition in fluidization and standpipe flow. Powder Technology. 124: 45-54. http://dx.doi.org/10.1016/S0032-5910(01)00471-5

Tumuluru, J.S., L.G. Tabil, Y. Song, K.L. Iroba and V. Meda. 2014. Griding energy and physical properties of chopped and hammer-milled barley, wheat, oat and canola straws. Biomass and Bioenergy 60: 58-67. http://dx.doi.org/10.1016/j.biombioe.2013.10.011

Vejahati, F., N. Mahinpey, N. Ellis and M.B. Nikoo. 2009. CFD simulation of gas–solid bubbling fluidized bed: A new method for adjusting drag law, Canadian Journal of Chemical Engineering. 87: 19-30. http://dx.doi.org/10.1002/cjce.20139

Wang, Q., T. Niemi, J. Peltola, S. Kallio, H. Yang, J. Lu and L. Wei. 2015. Particle size distribution in CPFD modeling of gas–solid flows in a CFB riser. Particuology 21: 107-117. http://dx.doi.org/10.1016/j.partic.2014.06.009

Yang, W. 2003. Particle characterization and dynamics, In Handbook of Fluidization and Fluid Particle Systems, ed. W. Yang, 1-27. New York, NY: Marcel Dekker Inc. http://dx.doi.org/10.1201/9780203912744.ch1